ChemComm

RSC Publishing

COMMUNICATION

View Article Online
View Journal | View Issue

Cite this: *Chem. Commun.*, 2013, **49**, 11430

Received 7th September 2013,
Accepted 14th October 2013

DOI: 10.1039/c3cc46862c

www.rsc.org/chemcomm

In vitro and *in vivo* imaging application of a 1,8-naphthalimide-derived Zn^{2+} fluorescent sensor with nuclear envelope penetrability†

Changli Zhang,[ab] Zhipeng Liu,[c] Yunling Li,[a] Weijiang He,*[a] Xiang Gao[d] and Zijian Guo*[a]

A newly developed fluorescent sensor, Naph-BPEA, shows a specific turn-on response to Zn^{2+} and can be excited by visible light. The *in situ* nuclear Zn^{2+} imaging in HeLa and HepG2 cells reveals the nuclear envelope penetrability of the sensor. The specific sensor location in a zebrafish larva was also demonstrated.

The subcellular Zn^{2+} imaging of specific compartments using sensors with specific intracellular distribution patterns is of great interest, since many subcellular organs are involved in Zn^{2+} homeostasis with variable roles.[1] For example, the nucleus has been correlated with intracellular Zn^{2+} transportation and storage,[2] and the Zn^{2+} storage protein metallothionein can be re-distributed from the cytoplasm to the nucleus during phase transition from G1 to S.[2a,3] Moreover, many nuclear proteins such as transcription factors, polymerases, and DNA remodeling factors cannot work properly without Zn^{2+}.[4] Understanding the roles of nuclear Zn^{2+} demands sensors with nuclear envelope penetrability to realize the *in situ* nuclear Zn^{2+} imaging. However, the Zn^{2+} sensors with nuclear envelope penetrability are rare so far, besides the genetically encoded FRET sensors developed by Palmer and coworkers.[2a] Small molecular Zn^{2+} sensors with nuclear envelope penetrability are also desirable due to their advantages such as a simple staining procedure, fine reproducibility, and high stability and sensitivity. Newport Green (diacetate form of cell membrane permeability functioning *via* intracellular hydrolysis) and Zinquin (UV excitable) are among the very few examples displaying an even distribution throughout the entire cell including the nucleus,[2b,5] however Zinquin is unable to enter the nucleus of numerous cell lines and cannot visualize the nuclear Zn^{2+} enhancement induced by Zn^{2+}/pyrithione incubation.[3b]

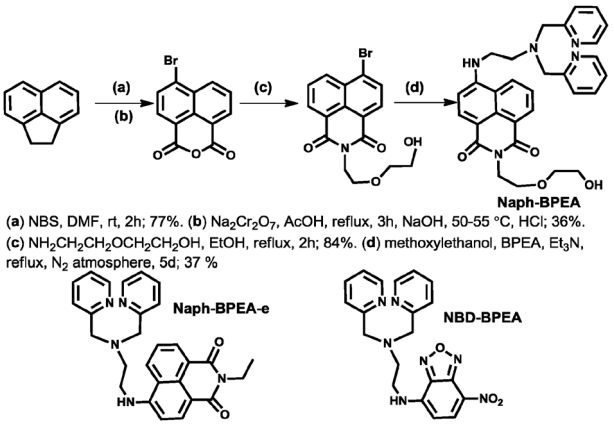

Scheme 1 Synthesis of **Naph-BPEA** and the chemical structures of **Naph-BPEA-e**, and **NBD-BPEA**.

Herein, we report a new turn-on fluorescent Zn^{2+} sensor with nucleus envelope penetrability, **Naph-BPEA** (Scheme 1). With the visible light excitability and cell membrane permeability, this sensor is able to realize not only the nuclear Zn^{2+} imaging but also the *in vivo* Zn^{2+} imaging in a zebrafish larva.

The new sensor was derived from 4-amino-1,8-naphthalimide (ANaph), an internal charge transfer (ICT) fluorophore with visible light excitability and medium quantum yield,[6] and its DNA targeting ability was expected to improve the nucleus localization of **Naph-BPEA**. In fact, the anion sensors based on ANaph are able to enter the nucleus.[7] The Zn^{2+} ionophore *N*,*N*′-bis(pyridin-2-ylmethyl)ethane-1,2-diamine (BPEA) was incorporated as the ICT donating group of the ANaph fluorophore. Its 2-(2-aminoethoxyl)ethanol moiety was introduced to improve the aqueous solubility of this sensor. **Naph-BPEA** was prepared from acenaphthene *via* a four step procedure with a total yield of 8.6% (Scheme 1, for details, please see the ESI†). Its analogue with the ethyl group replacing its 2-(2-aminoethoxyl)ethanol tail, **Naph-BPEA-e**, was also prepared (Scheme S2, ESI†).

Naph-BPEA emits in aqueous HEPES buffer (10 μM, 50 mM HEPES, 100 mM KNO_3, 1% DMSO, pH 7.2) with the emission and excitation maxima being at 546 and 450 nm, respectively.

[a] *State Key Laboratory of Coordination Chemistry, Coordination Chemistry Institute, School of Chemistry and Chemical Engineering, Nanjing University, Nanjing 210093, P. R. China. E-mail: heweij69@nju.edu.cn, zguo@nju.edu.cn; Fax: +86 25 83314502; Tel: +86 25 83597066*
[b] *Department of Chemistry, Nanjing Xiaozhuang College, Nanjing 210017, P. R. China*
[c] *Department of Chemistry, Liaocheng University, Liaocheng 252059, P. R. China*
[d] *Animal Model Research Center, Nanjing University, Nanjing 210061, P. R. China*

† Electronic supplementary information (ESI) available: Synthesis, spectroscopic studies, imaging results and experimental details. See DOI: 10.1039/c3cc46862c

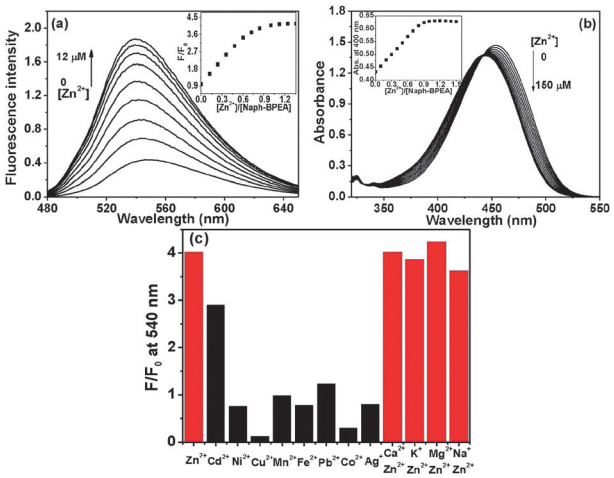

Fig. 1 Emission (a, 10 μM, λ_{ex}, 450 nm) and absorption (b, 100 μM) spectra of **Naph-BPEA** in HEPES buffer (50 mM, 100 mM KNO_3, pH 7.2) obtained upon titration with Zn^{2+} solution (1.2 mM for a, 10 mM for b) at 25 °C. The buffer contains 1% (for a) or 10% (for b) DMSO (v/v). Inset in (a): the titration profile based on the emission at 540 nm; inset in (b): the titration profile based on the absorbance at 400 nm. (c) A histogram of the emission enhancement factor (based on the emission at 540 nm) of **Naph-BPEA** (10 μM) induced by different metal cations in the same buffer of (a). Na^+, K^+, Ca^{2+}, Mg^{2+}, 1000 equiv., other metal cations, 1 equiv. λ_{ex} for (a) and (c) is 450 nm.

Upon Zn^{2+} titration, **Naph-BPEA** displays a linear emission enhancement with $[Zn^{2+}]_{total}$, and the emission enhancement factor is ~4 when the $[Zn^{2+}]_{total}$–[**Naph-BPEA**] ratio of 1 : 1 is attained. Even higher $[Zn^{2+}]_{total}$ does not lead to any further emission enhancement (Fig. 1a). UV titration of **Naph-BPEA** with Zn^{2+} exhibits an absorption hypsochromic shift from 453 to 442 nm, and the clear isosbestic point at 442 nm implies that only one zinc coordination process occurs upon Zn^{2+} titration (Fig. 1b). The titration profile based on the emission at 540 nm and that based on the absorbance at 400 nm both suggest a 1 : 1 Zn^{2+} binding stoichiometry of **Naph-BPEA**. The new set of signals appearing in the ^{1}H NMR spectrum of **Naph-BPEA** upon Zn^{2+} titration becomes the only set of signals when the $[Zn^{2+}]$–[**Naph-BPEA**] ratio of 1 : 1 is attained (Fig. S1, ESI†). This phenomenon also confirms the 1 : 1 Zn^{2+} binding stoichiometry. Moreover, the Zn^{2+}-induced signal shifts for protons of ANaph and BPEA moieties in the ^{1}H NMR spectrum suggest that all the N atoms of the BPEA moiety were directly involved in Zn^{2+} coordination. It is the direct Zn^{2+} coordination of the terminal amino group of BPEA that induced the blue shift of the ICT absorption band, since this amino group also acts as the ICT donating group of the ANaph fluorophore. In fact, Zn^{2+} titration also induces the minor emission blue shift (~10 nm). The dissociation constant of the Zn^{2+}–**Naph-BPEA** complex was estimated to be ~4 nM. The quantum yield of the Zn^{2+}–**Naph-BPEA** complex was determined to be 0.19 with NBD–$NHCH_3$ in acetonitrile as the reference.[8]

The specific Zn^{2+}-amplified fluorescence of **Naph-BPEA** was verified *via* screening the metal cations of interest (Fig. 1c). Except for Zn^{2+}, only Cd^{2+} and Pb^{2+} among the tested cations trigger the emission enhancement, with the respective factors of ~3- and 1.3-fold. Other tested cations do not affect **Naph-BPEA** emission distinctly, except for Cu^{2+} and Co^{2+} that induce the minor emission quenching. The intracellular Zn^{2+} sensing behavior of **Naph-BPEA** will not be interfered by Cd^{2+} and Pb^{2+} in the normal case due to the extremely low intracellular level of Cd^{2+} and Pb^{2+}. Moreover, the presence of cellular abundant Na^+, K^+, Ca^{2+} and Mg^{2+} (1000 equiv.) does not affect the Zn^{2+} sensing behavior of **Naph-BPEA**. It is proposed that the **Naph-BPEA** analogue with a specific azo-crownether or azo-cryptand as a Zn^{2+} chelator to combine with the ANaph fluorophore might be helpful in enhancing the sensing selectivity over Cd^{2+} and Pb^{2+}, since the radius of Zn^{2+} is smaller than those of the two cations. The stable emission of **Naph-BPEA** in the pH range from 6.5 to 9.0 indicates the pH-independent fluorescence of **Naph-BPEA** in physiological microenvironments (Fig. S3, ESI†). In addition, the detection limit (3σ/slope) of this sensor was determined to be 57 nM (Fig. S4, ESI†). All these suggest that this sensor might be a suitable candidate as an imaging agent for intracellular Zn^{2+}.

The intracellular distribution pattern and Zn^{2+} imaging ability of **Naph-BPEA** were investigated in living cells. The punctated cytosolic fluorescence pattern circling an internal dim area can be observed in the **Naph-BPEA**-stained HepG2 cells (Fig. S5, ESI†). When exogenous Zn^{2+} are introduced into the cells *via* $ZnSO_4$–pyrithione incubation (5 μM, 1 : 1), the entire cell turns fluorescent, and the former punctated region becomes even brighter. The following treatment by the membrane-permeable Zn^{2+} chelator TPEN (*N,N,N′,N′*-tetrakis(2-pyridylmethyl)ethylenediamine) results in a recovered dim image with the punctated fluorescence pattern becoming weaker than that before Zn^{2+} incubation (Fig. S5, ESI†). These results suggest that **Naph-BPEA** is an effective Zn^{2+} imaging agent with cell membrane permeability, and can be distributed throughout cells including the nucleus.

The nuclear envelope penetrability and nuclear Zn^{2+} imaging ability of **Naph-BPEA** were confirmed in the HeLa cells co-stained with **Naph-BPEA** and the nucleus dye Hoechst 33 342. The navy blue colour in the Hoechst channel image (λ_{ex}, 351 nm; band path 420–470, blue channel) of the stained cells shows the nucleus location (Fig. 2a). Imposing this image on the **Naph-BPEA** channel image (λ_{ex}, 488 nm, band path 500–600 nm, green channel) of the same cells confirms that the punctated fluorescence pattern in the green channel image locates in the cytoplasm, while the nucleus turns dim upon excitation at 488 nm (Fig. 2b and c). Upon Zn^{2+}–pyrithione incubation, the green channel image displays the total fluorescent cells (Fig. 2e). Co-localization *via* overlaying the green channel image on the blue channel image demonstrates the pale blue nucleus as the co-staining effect of **Naph-BPEA** and Hoechst 33 342, inferring the coexistence of labile Zn^{2+} and **Naph-BPEA** in the nucleus (Fig. 2f). The subsequent TPEN treatment resulted in the recovered dim nucleus and the weak cytosolic punctated fluorescence pattern (Fig. 2g and h). All these confirm that **Naph-BPEA** can be distributed throughout the cells including the nucleus. It is the low nuclear labile Zn^{2+} level that resulted in the initial dim nucleus, and the labile Zn^{2+} fluctuation in the nucleus induced by Zn^{2+}–pyrithione incubation and TPEN treatment can be visualized clearly using

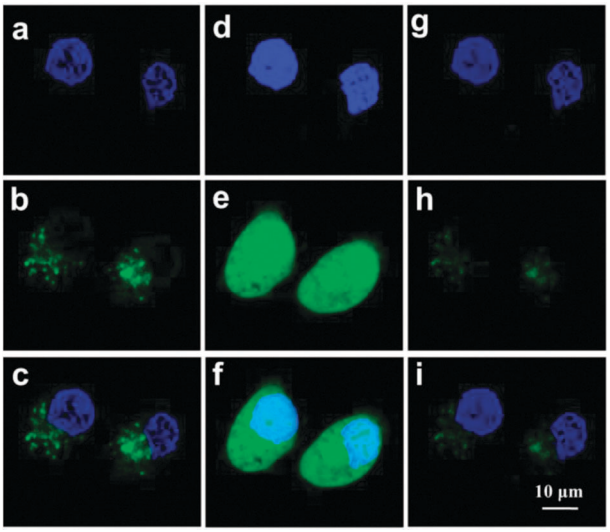

Fig. 2 Confocal fluorescence images of HeLa cells co-stained with Hoechst 33 342 (5 μg mL^{-1} in PBS, 10 min) and **Naph-BPEA** (5 μM in PBS, 20 min). (a–c): images of the co-stained cells; (d–f): images of the co-stained cells followed by Zn^{2+}–pyrithione incubation (5 μM, 1 : 1, 5 min); (g–i): images of Zn^{2+}-incubated cells treated further by TPEN (25 μM in PBS, 10 min). (a), (d) and (g): The Hoechst channel (blue channel, λ_{ex}, 351 nm, band path 420–470 nm) images; (b), (e) and (f): the **Naph-BPEA** channel (green channel, λ_{ex}, 488 nm, band path 500–600 nm) images; (c), (f) and (i): overlays of the related blue/green channel images.

Naph-BPEA. The intracellular distribution pattern of **Naph-BPEA** suggests the possibility of simultaneously monitoring labile Zn^{2+} levels in the nucleus and cytoplasm.

NBD-BPEA (Scheme 1) is a turn-on Zn^{2+} sensor developed similarly *via* incorporating BPEA as the ICT donating group of the ICT fluorophore 4-amino-7-nitro-2,1,3-benzoxadiazole (ANBD).[9] Co-localization imaging of HeLa cells co-stained with Hoechst 33 324 and **NBD-BPEA** disclosed that Zn^{2+} imaging *via* **NBD-BPEA** showed only the cytosolic punctated fluorescence pattern even upon Zn^{2+}–pyrithione incubation (Fig. S6, ESI†). With the identical Zn^{2+} chelator BPEA, **Naph-BPEA** and **NBD-BPEA** are expected to have a similar Zn^{2+} binding ability, and the dim nucleus upon Zn^{2+} incubation in the case of **NBD-BPEA** implies that there are no sensor molecules distributed in the nucleus. The different intracellular distribution patterns between **NBD-BPEA** and **Naph-BPEA** suggest that the DNA-targeting ANaph might be the origin for the nuclear envelope penetrability of **Naph-BPEA**. In fact, its analogue **Naph-BPEA-e** with the ethyl tail displays also the nuclear envelope penetrability (Scheme 1 and Fig. S7, ESI†). The nucleus penetrability of **Naph-BPEA** does not have evident impact on the cell viability, and the cells appear to show the normal morphology during the imaging process. The MTT assays disclosed that the cellular viability of HeLa and HepG2 cells after 48 h of **Naph-BPEA** incubation (5 μM) is 94.5 ± 2.0% and 98.5 ± 1.0%, respectively.

The nuclear Zn^{2+} imaging ability and nuclear envelope penetrability of **Naph-BPEA** inspire us to determine its *in vivo* Zn^{2+} imaging ability in a transparent zebrafish larva (5-day-old). The larva image obtained *via* **Naph-BPEA** staining displays the two zygomorphic fluorescent regions around its ventricle, similar to the image obtained *via* staining with a Zn^{2+} sensor **NBD-TPEA**.[10] Moreover, the additional fluorescent stream in the tail

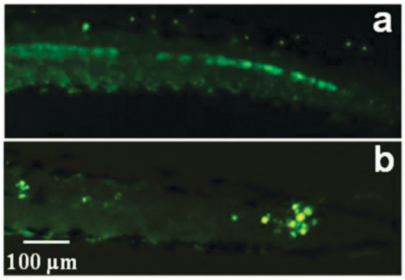

Fig. 3 Fluorescence images of a Zn^{2+}-fed 5-day-old zebrafish larva obtained by a fluorescence microscope. (a) The **Naph-BPEA**-stained larva (5 μM, 28.5 °C, 30 min); (b) the **NBD-TPEA**-stained larva (5 μM, 28.5 °C, 30 min).

was observed as the larva notochord (Fig. 3a). Such a stream is not visible if the larva is not Zn^{2+}-fed. Moreover, it cannot be observed by **NBD-TPEA** staining even when the larva is Zn^{2+}-fed (Fig. 3b). The Zn^{2+} imaging ability in the notochord of the zebrafish larva implies that **Naph-BPEA** can be a potential *in vivo* imaging agent for Zn^{2+} involved in the development of zebrafish.

In conclusion, a new Zn^{2+} fluorescent sensor, **Naph-BPEA**, was developed from 1,8-naphthalimide. Its nuclear envelope penetrability and specific Zn^{2+}-amplified fluorescence provide this sensor the ability to image nuclear Zn^{2+} in HeLa and HepG2 cells. The *in situ* nuclear Zn^{2+} imaging using this sensor is esterase-independent and can be accomplished by visible light excitation. This study also suggests that ANaph incorporation might be an effective strategy to devise a sensor with nuclear envelope penetrability.

We thank the National Basic Research Program of China (No. 2011CB935800) and the National Natural Science Foundation of China (No. 21271100, 21131003, 21021062, and 91213305) for financial support.

Notes and references

1 (*a*) S. L. Sensi, D. Ton-That, P. G. Sullivan, E. A. Jonas, K. R. Gee, L. K. Kaczmarek and J. H. Weiss, *Proc. Natl. Acad. Sci. U. S. A.*, 2003, **100**, 6157; (*b*) Y. Qin, P. J. Dittmer, J. G. Park, K. B. Jansen and A. E. Palmer, *Proc. Natl. Acad. Sci. U. S. A.*, 2011, **108**, 7351.
2 (*a*) J. G. Miranda, A. L. Weaver, Y. Qin, J. G. Park, C. I. Stoddard, M. Z. Lin and A. E. Palmer, *PLoS One*, 2012, **7**, e49371; (*b*) H. Hasse and D. Beyersmann, *Biochem. Biophys. Res. Commun.*, 2002, **296**, 923.
3 (*a*) K. Tsujikawa, T. Imai, M. Kakutani, Y. Kayamori, T. Mimura, N. Otaki, M. Kimura, R. Fukuyama and N. Shimizu, *FEBS Lett.*, 1991, **283**, 239; (*b*) P. Coyle, P. D. Zalewski, J. C. Philcox, I. J. Forbest, A. D. Ward, S. F. Lincoln, I. Mahadevan and A. M. Rofe, *Biochem. J.*, 1994, **303**, 781.
4 (*a*) C. Andreini, L. Banci, I. Bertini and A. Rosato, *J. Proteome Res.*, 2006, **5**, 3173; (*b*) C. Andreini, L. Banci, I. Bertini and A. Rosato, *J. Proteome Res.*, 2006, **5**, 196.
5 L. M. T. Canzoniero, D. M. Turetsky and D. W. Choi, *J. Neurosci.*, 1999, **19**, RC31.1.
6 S. Banerjee, E. B. Veale, C. M. Phelan, S. A. Murphy, G. M. Tocci, L. J. Gillespie, D. O. Frimannsson, J. M. Kelly and T. Gunnlaugsson, *Chem. Soc. Rev.*, 2013, **42**, 1601.
7 (*a*) E. B. Veale, D. O. Frimannsson, M. Lawler and T. Gunnlaugsson, *Org. Lett.*, 2009, **11**, 4040; (*b*) E. B. Veale and T. Gunnlaugsson, *J. Org. Chem.*, 2010, **75**, 5513.
8 S. Uchiyama, Y. Matsumura, A. P. de Silva and K. Iwai, *Anal. Chem.*, 2003, **75**, 5926.
9 W. Jiang, Q. Fu, H. Fan and W. Wang, *Chem. Commun.*, 2008, 259.
10 F. Qian, C. Zhang, Y. Zhang, W. He, X. Gao, P. Hu and Z. Guo, *J. Am. Chem. Soc.*, 2009, **131**, 1460.

